Contribution from the Chemistry Department, University of Guelph, Guelph, Ontario, Canada N1G 2W1,
Department of Chemistry, University of Glasgow, Glasgow G12 8QQ, Scotland, U.K.,
and Department of Chemistry, University of Western Ontario, London, Ontario, Canada N6A 5B7

Oxidative Addition of Thiocyanate to Coordinatively Unsaturated Trinuclear Clusters: Structures of $[Pt_3(SCN)(\mu_3\text{-}CO)(\mu\text{-dppm})_3]^+$ and $[Pd_3(\mu_3\text{-}S)(CN)(\mu\text{-dppm})_3]^+$ (dppm = $Ph_2PCH_2PPh_2$)

George Ferguson,*[1a] Brian R. Lloyd,[1b] Ljubica Manojlović-Muir,*[1c] Kenneth W. Muir,[1c]
and Richard J. Puddephatt*[1b]

Received May 13, 1986

Reaction of the cationic clusters $[M_3(\mu_3\text{-}CO)(\mu\text{-dppm})_3]^{2+}$ (**1a**, M = Pd; **1b**, M = Pt; dppm = $Ph_2PCH_2PPh_2$) with thiocyanate gives first $[M_3(SCN)(\mu_3\text{-}CO)(\mu\text{-dppm})_3]^+$ (**2a**, M = Pd; **2b**, M = Pt), and a further rearrangement then occurs when M = Pd to give $[M_3(\mu_3\text{-}S)(CN)(\mu\text{-dppm})_3]^+$ (**3a**, M = Pd). The reaction of **2a** to give **3a**, which follows first-order kinetics, leads to cleavage of the S–C bond of the thiocyanate ion, giving sulfide and cyanide and two of the Pd–Pd bonds of **2a**. Evidence is presented that inversion of the $Pd_3(\mu_3\text{-}S)$ unit of **3a** occurs rapidly in solution. The structures of $[\mathbf{2b}][PF_6]\cdot 2(CH_3)_2CO$ and $[\mathbf{3a}][SCN]\cdot 3C_2H_4Cl_2$ have been determined by X-ray diffraction. Crystals of the [**2b**] salt are monoclinic, space group $P2_1/n$, with a = 16.125 (1) Å, b = 26.622 (2) Å, c = 19.403 (1) Å, β = 104.45 (1)°, and Z = 4. R = 0.041 for 7057 independent structure amplitudes. The cation [**2b**] contains an equilateral triangle of platinum atoms [mean Pt–Pt = 2.623 (2) Å] edge-bridged by three dppm ligands and capped by a μ_3-CO group [Pt–C = 2.04 (1)–2.18 (1) Å]. The SCN^- anion caps the opposite face of the triangle, with the sulfur atom lying much closer to Pt(1) than to Pt(2) or Pt(3) [Pt–S = 2.656 (4), 3.380 (4), and 3.243 (4) Å]. Ionic and weakly covalent bonding models for the Pt–SCN interaction are discussed. Crystals of $[\mathbf{3a}][SCN]\cdot 3C_2H_4Cl_2$ are orthorhombic, space group $Pnma$, with four formula units in a unit cell of dimensions a = 24.110 (7), b = 21.652 (5), and c = 16.126 (3) Å. R = 0.047 for 3423 reflections with $I > 3\sigma(I)$. The cation [**3a**], disordered anion, and disordered solvent molecules all have crystallographic mirror symmetry. Cation [**3a**] has an isosceles triangle of Pd atoms [Pd(1)··Pd(2) = 3.508 (1) Å; Pd(2)–Pd(2)* = 2.579 (1) Å], edge bridged by three dppm ligands and capped by a lone S atom that lies 1.311 (3) Å above the Pd_3 plane and is equidistant from the Pd atoms [Pd–S = 2.297 (3) Å]. Distorted square-planar coordination at Pd(1) is completed by a CN ligand [Pd–C = 2.059 (12) Å]. The crystallographic mirror plane passes through Pd(1), the S atom, the CN ligand, and a CH_2 of a dppm ligand.

Introduction

Bridging sulfide complexes containing $M_2(\mu_2\text{-}S)$ or $M_3(\mu_3\text{-}S)$ linkages are often very stable and can be formed from organosulfur precursors as well as from conventional sources of sulfide.[2,3] Some precursors that form sulfides by cleavage of S—C or S═C bonds include RSH, R_2S, CR_2CR_2S, CS_2, COS, and RNCS, where R = alkyl or aryl.[2–8] In some cases, intermediates have been isolated that aid in understanding of the mechanisms of reaction.[6,8] This work is significant since analogous mechanisms are possible in the poisoning of platinum and palladium catalysts by organosulfur impurities in feedstocks.

The complex cations $[M_3(\mu_3\text{-}CO)(\mu\text{-dppm})_3]^{2+}$ (**1a**, M = Pd; **1b**, M = Pt; dppm = $Ph_2PCH_2PPh_2$) can act as models for reactions occurring at the 3-fold sites on a palladium or platinum surface[9–12] and so their reactions with inorganic and organic sulfur-containing compounds are of interest. In this paper reactions with the thiocyanate ion are reported. Thiocyanate has been an important ligand in coordination chemistry due to the multiplicity of bonding modes that can be adopted, but we know of no published reports of its cleavage by transition-metal complexes to sulfide and cyanide.[2,3,13] We find that such cleavage occurs readily on reaction of thiocyanate with **1a** but much more slowly with **1b**, and details of these reactions are given below.

Scheme I

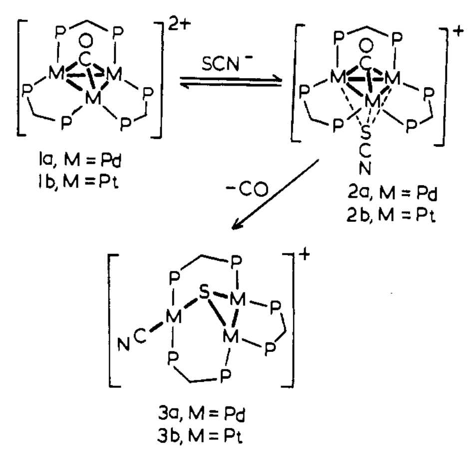

Results and Discussion

The major chemical results are given in Scheme I. Thiocyanate first adds to the vacant site below the M_3 triangle of **1** to give **2**, and then, when M = Pd, a further transformation occurs with cleavage of the S–C bond and loss of CO to give **3a**.

Formation and Structures of the Thiocyanate Complexes 2a and 2b. Reaction of $[\mathbf{1b}][PF_6]_2$ with excess thiocyanate in acetone solution gave [**2b**][SCN] and this could easily be reconverted to the hexafluorophosphate salt $[\mathbf{2b}][PF_6]$ by anion exchange. The structure of $[\mathbf{2b}][PF_6]$ was determined by diffraction methods, using crystals obtained from acetone/pentane solution.

---

(1) (a) University of Guelph. (b) University of Western Ontario. (c) University of Glasgow.
(2) Vahrenkamp, H. *Angew. Chem., Int. Ed. Engl.* **1975**, *14*, 322. *Sulfur*; Müller, A., Krebs, B., Eds.; Elsevier: Amsterdam, 1984; pp 121–139.
(3) Adams, R. D.; Horváth, I. T. *Prog. Inorg. Chem.* **1985**, *33*, 127.
(4) Hawling, W. M.; Walker, A.; Woitzik, A. *J. Chem. Soc., Chem. Commun.* **1983**, 11.
(5) Scherer, O. J.; Konrad, R.; Guggolz, E.; Ziegler, M. L. *Chem. Ber.* **1983**, *116*, 2676.
(6) Ebner, M.; Otto, H.; Werner, H. *Angew. Chem., Int. Ed. Engl.* **1985**, *24*, 518.
(7) Werner, H.; Leonhard, K.; Kolb, O.; Röttinger, E.; Vahrenkamp, H. *Chem. Ber.* **1980**, *113*, 1654.
(8) Adams, R. D.; Dawoodi, Z.; Foust, D. F.; Segmüller, B. E. *Organometallics* **1983**, *2*, 315.
(9) Manojlović-Muir, Lj.; Muir, K. W.; Lloyd, B. R.; Puddephatt, R. J. *J. Chem. Soc., Chem. Commun.* **1983**, 1336.
(10) Lloyd, B. R.; Puddephatt, R. J. *Inorg. Chim. Acta* **1984**, *90*, L77.
(11) Manjlović-Muir, Lj.; Muir, K. W.; Lloyd, B. R.; Puddephatt, R. J. *J. Chem. Soc., Chem. Commun.* **1985**, 536.
(12) Ferguson, G.; Lloyd, B. R.; Puddephatt, R. J. *Organometallics* **1986**, *5*, 344.
(13) Burmeister, J. L. *Chemistry and Biochemistry of Thiocyanic Acid and its Derivatives*; Newman, A. A., Ed.; Academic: New York, 1975; Chapter 2.

0020-1669/86/1325-4190$01.50/0

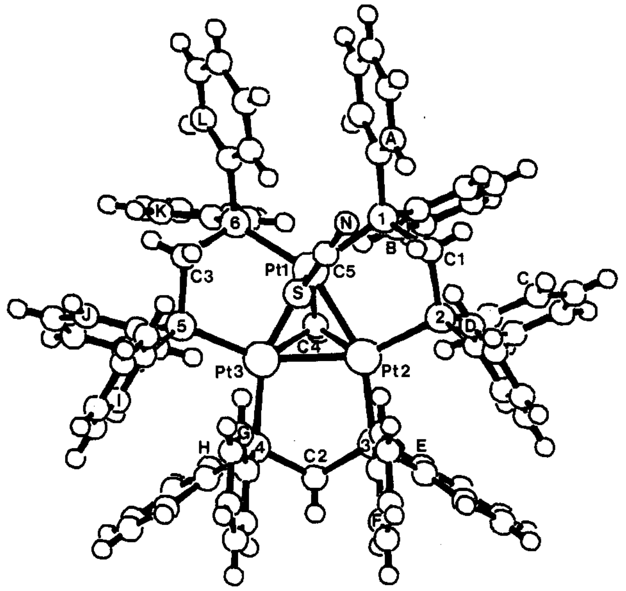

Figure 1. The $[Pt_3(SCN)(\mu_3\text{-}CO)(\mu\text{-}dppm)_3]^+$ cation viewed along the normal to the Pt_3 triangle. For clarity only an abbreviated form of the atom-numbering scheme is shown. Phenyl carbon atoms are numbered cyclically as C(n1)–C(n6), n = A–L, with C(n1) attached to phosphorus. Only the label n of C(n2) is indicated for each ring. The six phosphorus atoms are indicated by their serial numbers 1–6.

The crystals are built of **[2b]** cations, $[PF_6]^-$ anions, and acetone solvate molecules. The anions and the solvate molecules are subject to a high degree of thermal motion.

The structure of the cation **[2b]** (Figure 1) is based on an equilateral triangle of platinum atoms edge-bridged by dppm ligands. One face of the Pt_3 triangle is capped by a triply bridging carbonyl ligand. These structural features are common to **[2b]** and the parent cluster cation **[1b]**.[12] The mean Pt–Pt bond length in **[2b]** of 2.623 (2) Å (Table I) agrees with that in **[1b]** [2.634 Å], and both are in the range considered typical of Pt–Pt single bonds. However, the individual Pt–Pt distances in **[2b]** (Table I) are more regular than those in **[1b]**, which vary from 2.613 (1) to 2.650 (1) Å. In **[2b]** the μ_3-CO ligand is closer to Pt(1) than it is to Pt(2) or Pt(3) [respective Pt–C(4) distances are 2.04 (1), 2.17 (1) and 2.18 (1) Å], whereas in **[1b]** the $Pt_3(\mu_3\text{-}CO)$ linkage is more symmetric [Pt–C = 2.08 (1)–2.10 (1) Å].

The other face of the Pt_3 triangle in **[2b]** is occupied by a linear SCN^- ligand, with the sulfur atom directed toward the metal atoms. The Pt(2)···S and Pt(3)···S distances [3.380 (4) and 3.243 (4) Å] are clearly too long to represent bonds. The Pt(1)–S distance [2.656 (4) Å] is much shorter, but is still abnormally long for a covalent Pt–SCN bond: a survey of such distances[14] yielded values in the range 2.31–2.41 Å, the longest being 2.408 (4) Å in $[Pt_2Cl_2(\mu\text{-}SCN)_2(P\text{-}n\text{-}Pr_3)_2]$.[15] The difference [$\Delta r$ = 0.30 Å] between the Pt(1)–S distance in **[2b]** and the mean value for other Pt–SCN bond lengths [2.36 Å] implies a fractional bond order n of 0.3, according to the Pauling formula $\Delta r = -0.60 \log n$.[16] We also note that the Pt(1)–S–C(5) angle of 111.5 (7)° in **[2b]** shows little difference from the values of 103–110° found in other Pt–SCN complexes.

Although complexes based on capped $M_3(\mu_3\text{-}dppm)_3$ cores have been described for M = Cu[17] and Ag,[18] the closest analogy with the weak attachment of SCN^- to the platinum cluster in **[2b]** is found in the related palladium cluster cations $[Pd_3X(\mu_3\text{-}CO)(\mu\text{-}$

Table I. Selected Distances (Å) and Angles (deg) for $[Pt_3(SCN)(\mu_3\text{-}CO)(\mu\text{-}dppm)_3][PF_6]\cdot 2(CH_3)_2CO$

Bond Lengths

Pt(1)–Pt(2)	2.620 (1)	Pt(1)–Pt(3)	2.625 (1)
Pt(1)–P(1)	2.313 (4)	Pt(1)–P(6)	2.306 (4)
Pt(1)–C(4)	2.042 (13)	Pt(2)–Pt(3)	2.623 (1)
Pt(2)–P(2)	2.294 (4)	Pt(2)–P(3)	2.271 (4)
Pt(2)–C(4)	2.165 (13)	Pt(3)–P(4)	2.280 (4)
Pt(3)–P(5)	2.280 (4)	Pt(3)–C(4)	2.175 (13)
P(1)–C(1)	1.823 (13)	P(1)–C(A1)	1.822 (4)
P(1)–C(B1)	1.827 (4)	P(2)–C(1)	1.840 (13)
P(2)–C(C1)	1.825 (4)	P(2)–C(D1)	1.822 (4)
P(3)–C(2)	1.876 (14)	P(3)–C(E1)	1.820 (4)
P(3)–C(F1)	1.814 (4)	P(4)–C(2)	1.821 (14)
P(4)–C(G1)	1.818 (4)	P(4)–C(H1)	1.826 (4)
P(5)–C(3)	1.850 (14)	P(5)–C(I1)	1.822 (4)
P(5)–C(J1)	1.803 (4)	P(6)–C(3)	1.844 (14)
P(6)–C(K1)	1.821 (4)	P(6)–C(L1)	1.821 (4)
S–C(5)	1.553 (19)	O–C(4)	1.165 (14)
N–C(5)	1.18 (2)		

Closest Contacts of the $Pt_3(\mu\text{-}dppm)_3$ Unit with the SCN and μ_3-CO Groups

Pt(1)···S	2.656 (4)	S···C(3)	3.602 (14)
Pt(2)···S	3.380 (4)	C(5)···C(1)	3.568 (20)
Pt(3)···S	3.243 (4)	C(5)···H(1A)	2.75
Pt(1)···C(5)	3.533 (18)	C(5)···H(L6)	2.80
Pt(1)···O	3.060 (9)	C(4)···P(1)	3.602 (13)
Pt(2)···O	3.045 (9)	C(4)···P(6)	3.569 (13)
Pt(3)···O	3.045 (9)	C(4)···H(B2)	2.75

Bond Angles

Pt(2)–Pt(1)–Pt(3)	60.0 (1)	Pt(2)–Pt(1)–P(1)	94.1 (1)
Pt(2)–Pt(1)–P(6)	153.5 (1)	Pt(2)–Pt(1)–C(4)	53.6 (4)
Pt(3)–Pt(1)–P(1)	154.1 (1)	Pt(3)–Pt(1)–P(6)	93.6 (1)
Pt(3)–Pt(1)–C(4)	53.8 (4)	P(1)–Pt(1)–P(6)	112.1 (2)
P(1)–Pt(1)–C(4)	111.4 (4)	P(6)–Pt(1)–C(4)	110.2 (4)
Pt(1)–Pt(2)–Pt(3)	60.1 (1)	Pt(1)–Pt(2)–P(2)	95.3 (1)
Pt(1)–Pt(2)–P(3)	155.0 (1)	Pt(1)–Pt(2)–C(4)	49.4 (4)
Pt(3)–Pt(2)–P(2)	153.2 (1)	Pt(3)–Pt(2)–P(3)	95.1 (1)
Pt(3)–Pt(2)–C(4)	53.0 (4)	P(2)–Pt(2)–P(3)	108.4 (2)
P(2)–Pt(2)–C(4)	120.3 (4)	P(3)–Pt(2)–C(4)	119.6 (4)
Pt(1)–Pt(3)–Pt(2)	59.9 (1)	Pt(1)–Pt(3)–P(4)	155.0 (1)
Pt(1)–Pt(3)–P(5)	95.8 (1)	Pt(1)–Pt(3)–C(4)	49.3 (4)
Pt(2)–Pt(3)–P(4)	95.5 (1)	Pt(2)–Pt(3)–P(5)	153.5 (2)
Pt(2)–Pt(3)–C(4)	52.6 (4)	P(4)–Pt(3)–P(5)	107.3 (2)
P(4)–Pt(3)–C(4)	121.1 (4)	P(5)–Pt(3)–C(4)	120.8 (4)
Pt(1)–P(1)–C(1)	106.4 (5)	Pt(1)–P(1)–C(A1)	120.4 (2)
Pt(1)–P(1)–C(B1)	116.7 (2)	C(1)–P(1)–C(A1)	104.5 (5)
C(1)–P(1)–C(B1)	104.9 (5)	C(A1)–P(1)–C(B1)	102.5 (2)
Pt(2)–P(2)–C(1)	110.3 (5)	Pt(2)–P(2)–C(C1)	116.2 (2)
Pt(2)–P(2)–C(D1)	116.9 (2)	C(1)–P(2)–C(C1)	105.4 (5)
C(1)–P(2)–C(D1)	103.9 (5)	C(C1)–P(2)–C(D1)	102.9 (2)
Pt(2)–P(3)–C(2)	110.1 (5)	Pt(2)–P(3)–C(E1)	117.0 (2)
Pt(2)–P(3)–C(F1)	116.1 (2)	C(2)–P(3)–C(E1)	101.0 (5)
C(2)–P(3)–C(F1)	103.8 (5)	C(E1)–P(3)–C(F1)	107.0 (2)
Pt(3)–P(4)–C(2)	109.6 (5)	Pt(3)–P(4)–C(G1)	115.1 (2)
Pt(3)–P(4)–C(H1)	115.4 (2)	C(2)–P(4)–C(G1)	104.9 (5)
C(2)–P(4)–C(H1)	101.9 (5)	C(G1)–P(4)–C(H1)	108.6 (2)
Pt(3)–P(5)–C(3)	110.9 (5)	Pt(3)–P(5)–C(I1)	114.9 (2)
Pt(3)–P(5)–C(J1)	116.3 (2)	C(3)–P(5)–C(I1)	104.2 (5)
C(3)–P(5)–C(J1)	106.1 (5)	C(I1)–P(5)–C(J1)	103.4 (2)
Pt(1)–P(6)–C(3)	107.0 (5)	Pt(1)–P(6)–C(K1)	114.7 (2)
Pt(1)–P(6)–C(L1)	120.5 (2)	C(3)–P(6)–C(K1)	107.6 (5)
C(3)–P(6)–C(L1)	100.0 (5)	C(K1)–P(6)–C(L1)	105.4 (2)
P(1)–C(1)–P(2)	112.0 (7)	P(3)–C(2)–P(4)	111.0 (7)
P(5)–C(3)–P(6)	111.3 (7)	Pt(1)–C(4)–Pt(2)	77.0 (5)
Pt(1)–C(4)–Pt(3)	76.9 (5)	Pt(1)–C(4)–O	143.8 (11)
Pt(2)–C(4)–Pt(3)	74.4 (5)	Pt(2)–C(4)–O	129.8 (10)
Pt(3)–C(4)–O	128.9 (10)	S–C(5)–N	179.8 (21)

Deviations from the Plane Defined by the Atoms Pt(1), Pt(2), and Pt(3)

P(1)	−0.050 (3)	O	−2.647 (9)
P(2)	0.438 (3)	N	4.15 (2)
P(3)	0.125 (4)	C(1)	0.96 (1)
P(4)	0.197 (4)	C(2)	−0.49 (1)
P(5)	0.437 (4)	C(3)	0.91 (1)
P(6)	−0.111 (3)	C(4)	−1.49 (1)
S	2.569 (4)	C(5)	3.46 (2)

---

(14) The CSSR programs were used to scan the Cambridge Structural Database. See: *CSSR Manual*, 3rd ed.; Daresbury, England, 1985.

(15) Gregory, U. A.; Jarvis, J. A. J.; Kilbourn, B. T.; Owston, P. G. *J. Chem. Soc. A* **1970**, 2770.

(16) Pauling, L. *The Nature of the Chemical Bond*, 3rd ed.; Cornell University Press: Ithica, NY, 1960; p 255.

(17) Ho, D. M.; Bau, R. *Inorg. Chem.* **1983**, *22*, 4079 and references therein.

(18) Aly, A. A. M.; Neugebauer, D.; Orama, O.; Schubert, U.; Schmidbauer, H. *Angew. Chem., Int. Ed. Engl.* **1978**, *17*, 125. Schubert, U.; Neugebauer, D.; Aly, A. A. M. *Z. Anorg. Allg. Chem.* **1980**, *464*, 217.

dppm)$_3$]$^+$ ([**4a**], X = $CF_3CO_2^-$; [**4b**], X = Cl^-; [**4c**], X = I^-).[9,11,19] These cations have latitudinal [$Pd_3(\mu_3$-CO)(μ-dppm)$_3$] cores similar to those of [**1b**] and [**2b**], with a loosely bound anion X straddling the Pd_3 triangle on the side opposite to carbonyl. In [**4a**] one $CF_3CO_2^-$ oxygen atom is 2.83 (1) Å from Pd(1), whereas the other is 2.77 (1) and 2.92 (2) Å from Pd(2) and Pd(3). In [**4b**] the finer structural details are obscured by Cl/CO disorder. [**4c**], however, is ordered, and its I^- anion is nearly equidistant from the metal atoms [Pd–I = 2.951 (1)–3.084 (1) Å]. Comparing the Pd–O and Pd–I distances in [**4a**] and [**4c**] with typical covalent Pd–O and Pd–I bond lengths [2.1 and 2.6 Å],[20] one may tentatively conclude that the attachment of the $CF_3CO_2^-$ anion to the palladium atoms in [**4a**] is relatively weak, whereas the binding of I^- in [**4c**] is stronger and indeed is comparable in strength to the SCN^- binding in [**2b**]. The species [**2b**] and [**4a**]–[**4c**] could be regarded as associations of [$M_3(\mu_3$-CO)(μ-dppm)$_3$]$^{2+}$ and X^- ions held together by purely electrostatic forces. This view is perhaps most compelling for [**4a**], whereas for [**2b**] and [**4c**] the case for some covalent component in the bonding between the anion and the cluster is harder to ignore.

A molecular orbital treatment of bonding in complexes containing a latitudinal [$M_3(\mu_3$-CO)P_6]$^{2+}$ core has shown that the 42 electrons contributed by the metal and ligand donor atoms are just sufficient to fill completely all the bonding skeletal orbitals.[21] Any additional electron donation from X^- might then lead to population of antibonding skeletal molecular orbitals, for which there is no evidence in the structures of [**2b**] and [**4a**]–[**4c**], or could be accommodated in ligand π^*-acceptor orbitals.[22] This latter possibility has been discussed[23] in the context of the 44-electron [$Pt_3(CO)_6$]$^{2-}$ species and is not obviously precluded for the [$M_3(\mu_3$-CO)P_6]$^{2+}$ cation, despite its relative poverty in π-acid ligands. It is also possible that donation of electron density into the vacant $6p_z$ orbitals of platinum could occur. There is an A_1 combination of $6p_z$ orbitals that could lead to formation of an $M_3(\mu_3$-X) group,[21] but it is also possible that just one $6p_z$ orbital could be involved to give a terminal MX group. Such an interaction would be weak because the $6p_z$ orbitals are at high energy[21–23] and need not affect the Pt–Pt bond strength to a significant degree.

The structural similarities between [**1b**], [**2b**], and [**4a**]–[**4c**] extend to the μ-dppm conformations, and these in turn dictate the steric environment of the capping ligands. In all these complexes the phosphorus atoms lie only approximately in the plane of the metal atoms [e.g., see Table I]. In general the M_2P_2C rings adopt more or less distorted C_s envelope conformations, with the methylene carbon atoms at the flap and P–Pt–Pt–P torsion angles near zero (e.g. 12.3 (2), 1.8 (2), and −13.9 (2)° across Pt(1)–Pt(2), Pt(2)–Pt(3), and Pt(1)–Pt(3) in [**2b**]). In all cases two methylene groups lie on the opposite side of the M_3 plane from the third. Thus, in [**2b**] the SCN^- anion occupies a hydrophobic cavity lined by methylenic carbon atoms C(1) and C(3), and by phenyl rings A, D, F, G, I, and L (Figure 2a). The shortest $SCN^-\cdots$ cavity contacts (Table I) involve ring L and the methylenic groups and are comparable with the sum of the appropriate van der Waals radii. They do not suggest that the closer approach of SCN^- to Pt(1) arises from steric constraints. On the opposite side of the Pt_3 triangle the μ_3-CO ligand lies in a cavity defined by the C(2) methylene group and rings B, C, E, H, J, and K. Again, neither the shape of the cavity (Figure 2b) nor the contacts between μ_3-CO and the cavity walls (Table I) explain the irregularities in the Pt–C(4) distances. In [**4a**] and [**4c**] the bulky $CF_3CO_2^-$ and I^- capping groups occupy cavities defined by two methylene and six phenyl groups, similar to that occupied by SCN^- in [**2b**], whereas in [**1b**] the corresponding cavity is occupied by μ_3-CO. In [**4b**] the disordered Cl and μ_3-CO groups show no site preference, presumably because of their similar size.

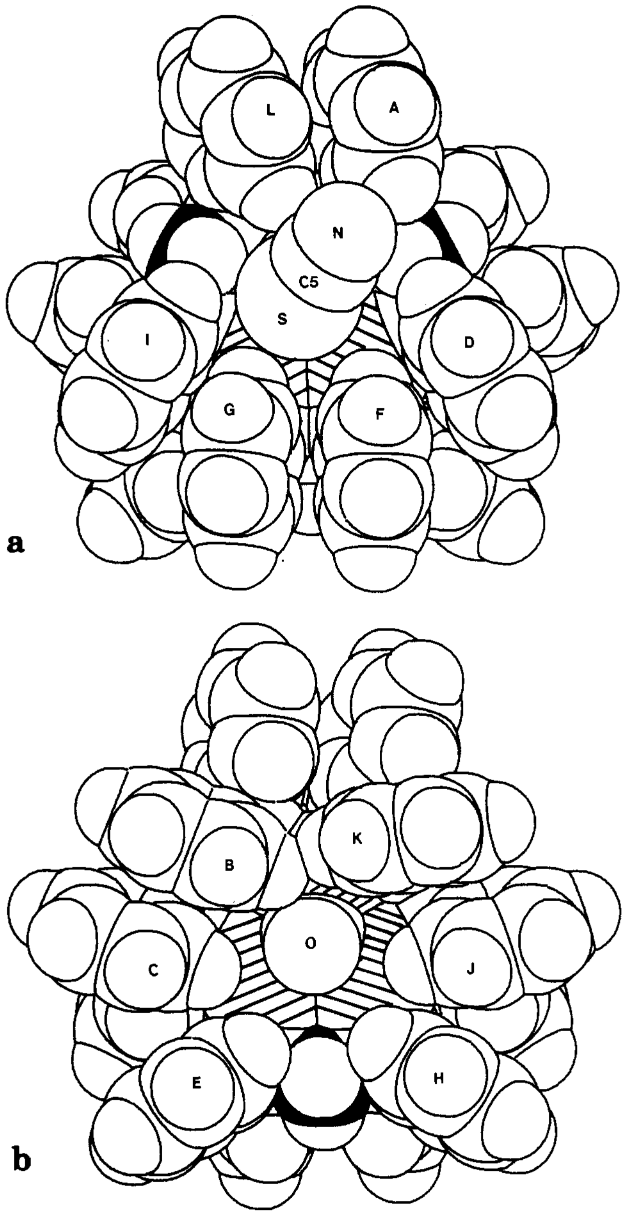

Figure 2. (a) View of a space-filling model of the [$Pt_3(SCN)(\mu_3$-CO)(μ-dppm)$_3$]$^+$ cation showing the environment of the thiocyanate anion. The direction of view is identical with that of Figure 1. (b) Environment of the μ_3-CO group. The model has been rotated 180° about the axis through Pt(1) and the midpoint of Pt(2)–Pt(3) relative to the view shown in part a. Platinum atoms are crosshatched. Methylene carbon atoms are shaded.

The greater interaction of Pt(1) with the capping ligands in [**2b**] is reflected in a slight irregularity in the Pt–P distances. The mean Pt–P bond length for Pt(2) and Pt(3) [2.281 (5) Å] agrees with that found in [**1b**] [2.282 Å], whereas the mean Pt(1)–P distance [2.310 (4) Å] is slightly larger. More surprisingly, the S–C(5) bond [1.55 (2) Å] is short compared both with values in Pt–SCN complexes [1.62–1.69 Å][14] and with those in uncomplexed SCN^- anions [typically 1.60–1.70 Å].[24] Evidently this bond is not activated in [**2b**], although the corresponding bond in [**2a**] is broken during formation of [**3a**].

---

(19) Manojlović-Muir, Lj.; Muir, K. W., unpublished results.

(20) Ukhin, L. Y., Dolgopolova, N. A.; Kuz'mina, L. G.; Struchkov, Y. T. *J. Organomet. Chem.* **1981**, *210*, 263. Hirschin, A. S.; Musker, W. K.; Olmstead, M. M.; Dallas, J. L. *Inorg. Chem.* **1981**, *20*, 1702.

(21) Mealli, C. *J. Am. Chem. Soc.* **1985**, *107*, 2245.

(22) Evans, D. G.; Mingos, D. M. P. *J. Organomet. Chem.* **1982**, *240*, 321.

(23) Lauher, J. W. *J. Am. Chem. Soc.* **1978**, *100*, 5305. Evans, J. *J. Chem. Soc., Dalton Trans.* **1980**, 1005. Evans, D. G.; Hughes, G. R.; Mingos, D. M. P.; Basset, J. M.; Welch, A. J. *J. Chem. Soc., Chem. Commun.* **1980**, 1255. Underwood, D. J.; Hoffman, R.; Tatsumi, K.; Nakamura, A.; Yamamoto, Y. *J. Am. Chem. Soc.* **1985**, *107*, 5968.

(24) Sakamaki, T.; Iitaka, Y.; Nawata, Y. *Acta Crystallogr., Sect. B: Struct. Crystallogr. Cryst. Chem.* **1977**, *B33*, 52; Akers, C.; Peterson, S. W.; Willett, R. D. *Acta Crystallogr., Sect. B: Struct. Crystallogr. Cryst. Chem.* **1968**, *B24*, 1125.

Table II. Principal Dimensions in the Cation **3a**

	Distances, Å		
Pd(1)–S(1)	2.297 (3)	P(1)–C(21)	1.804 (9)
Pd(1)–P(1)	2.320 (2)	P(2)–C(2)	1.827 (9)
Pd(1)–C(1)	2.059 (12)	P(2)–C(31)	1.816 (9)
Pd(2)–S(1)	2.297 (3)	P(2)–C(41)	1.801 (9)
Pd(2)–P(2)	2.297 (2)	P(3)–C(3)	1.840 (8)
Pd(2)–P(3)	2.270 (2)	P(3)–C(51)	1.831 (9)
Pd(2)–Pd(2*)	2.579 (1)	P(3)–C(61)	1.806 (9)
P(1)–C(2)	1.862 (9)	N(1)–C(1)	1.034 (18)
P(1)–C(11)	1.825 (9)		
	Angles, deg		
S(1)–Pd(1)–P(1)	92.21 (6)	C(2)–P(2)–C(41)	102.7 (4)
S(1)–Pd(1)–C(1)	176.0 (4)	C(31)–P(2)–C(41)	103.9 (4)
P(1)–Pd(1)–C(1)	88.40 (8)	Pd(2)–P(3)–C(3)	110.8 (4)
S(1)–Pd(2)–P(2)	98.29 (8)	Pd(2)–P(3)–C(51)	113.4 (3)
S(1)–Pd(2)–P(3)	149.86 (8)	Pd(2)–P(3)–C(61)	119.1 (3)
P(2)–Pd(2)–P(3)	110.29 (9)	C(3)–P(3)–C(51)	103.3 (4)
Pd(1)–S(1)–Pd(2)	99.6 (1)	C(3)–P(3)–C(61)	103.9 (5)
Pd(1)–P(1)–C(2)	119.1 (3)	C(51)–P(3)–C(61)	104.8 (4)
Pd(1)–P(1)–C(11)	105.0 (3)	P(1)–Pd(1)–P(1*)	162.1 (1)
Pd(1)–P(1)–C(21)	118.5 (3)	Pd(2*)–Pd(2)–S(1)	55.85 (5)
C(2)–P(1)–C(11)	103.0 (4)	Pd(2*)–Pd(2)–P(2)	154.08 (7)
C(2)–P(1)–C(21)	103.7 (4)	Pd(2*)–Pd(2)–P(3)	94.99 (6)
C(11)–P(1)–C(21)	105.7 (4)	Pd(2)–S(1)–Pd(2*)	68.30 (9)
Pd(2)–P(2)–C(2)	108.8 (3)	P(3)–C(3)–P(3*)	107.8 (6)
Pd(2)–P(2)–C(31)	110.6 (3)	Pd(1)–C(1)–N(1)	180 (1)
Pd(2)–P(2)–C(41)	125.6 (3)	P(1)–C(2)–P(2)	114.2 (5)
C(2)–P(2)–C(31)	102.7 (4)		

[a] Coordinates for the atoms marked with an asterisk are obtained from the coordinate list by applying the following transformation: *x*, 0.5 – *y*, *z*.

The $^{31}P\{^1H\}$ and $^{195}Pt\{^1H\}$ NMR spectra of [**2b**][PF_6] each contained single resonances showing that, on the NMR time scale, all ^{31}P and ^{195}Pt atoms are equivalent. Thus, if the structure in solution is the same as in the solid state, the molecule must be fluxional and the linear SCN^- ion must undergo a rapid precession within the cavity to cause effective equivalence of ^{31}P and ^{195}Pt atoms. This is not surprising since the Pt···S bonds are obviously weak. The asymmetric ν(SCN) stretching frequency for **2b** was 2070 cm^{-1}, only slightly higher than for ionic thiocyanate [e.g. KNCS has ν(NCS) = 2053 cm^{-1}] and lower than for covalent Pt–SCN complexes for which ν(NCS) > 2100 cm^{-1}, again consistent with only weak covalency in the Pt_3(SCN) bond.[13]

There is good evidence that reaction of **1a** with thiocyanate initially gives the analogous palladium complex **2a**, but this complex could not be crystallized in pure form due to its rearrangement to **3a**. Evidence for **2a** is as follows. Addition of 1 equiv of SCN^- to [**1a**][CF_3CO_2]$_2$ in acetone caused a shift in the ^{31}P NMR signal from $\delta = -12.7$ to $\delta = -11.3$, and in the UV-visible absorption maximum from 490 to 473 nm, which may be compared with similar shifts to −11.8 ppm and 459 nm, respectively,[11] on formation of $[Pd_3Br(\mu_3\text{-CO})(\mu\text{-dppm})_3]^+$.

The reaction of **2a** to give **3a** could be monitored conveniently by UV-visible spectroscopy. Isosbestic points were maintained at 435 and 335 nm, and the reaction followed good first-order kinetics with $k_1 = 2.2 \times 10^{-5}\ s^{-1}$ in methanol at 22 °C. The rate was not affected by the presence of excess thiocyanate.

Formation and Structure of Complex 3a. The complex [**3a**][SCN] was prepared by reaction of [**1a**][CF_3CO_2]$_2$ with excess thiocyanate. Recrystallization from dichloroethane afforded crystals of what proved to be [**3a**][SCN]·$3C_2H_4Cl_2$, whose structure was established by X-ray diffraction. The structure contains [**3a**] cations lying on a crystallographic mirror plane, SCN^- anions, and solvent molecules disordered about the mirror planes.

The cation **3a** (Figure 3a,b; Table II) lies about a crystallographic mirror plane (atoms C(3), S(1), Pd(1), C(1), N(1), on the mirror), and the structure is based on an isosceles triangle of Pd atoms, edge bridged by three dppm ligands, with the face of the triangle capped by a lone S atom, which is 1.311 (3) Å above one Pd_3 plane and equidistant (Pd–S = 2.297 (3) Å) from the Pd atoms. There is one Pd–Pd bond (Pd(2)–Pd(2*) = 2.579(1) Å) across the mirror plane; essentially identical Pd–Pd distances (2.576–2.610 Å) are found in $[Pd_3(\mu_3\text{-CO})(\mu\text{-dppm})_3][CF_3CO_2]_2$.[9-11] The other Pd···Pd distance in **3a** (Pd(1)···Pd(2) = 3.508 (1) Å) is too long to be considered bonding. Coordination at Pd(1) is distorted square planar with two trans phosphines (Pd(1)–P(1) = 2.320 (2) Å, P(1)–Pd(1)–P(1*) = 162.1 (1)°) and trans S and CN ligands (Pd–C = 2.059 (12) Å, S(1)–Pd(1)–C(1) 176.0 (4)°). Pd(2) is also four-coordinate, with geometry similar to that found in related *triangulo*-triplatinum and -tripalladium structures[9-12] and with P(2)–Pd(2)–P(3) = 110.3 (1)°. The six-membered ring Pd(1), S(1), Pd(2), P(2), C(2), and P(1) has a slightly twisted boat conformation, with S(1) +1.425 (3) Å and C(2) +0.756(9) Å from the Pd_2P_2 plane. The five-membered ring Pd(2), Pd(2*), P(3*), C(3), and P(3) has an envelope conformation with C(3) +0.747 (12) Å and S(1) +0.271 (3) Å from the Pd_2P_2 plane; i.e., the three methylene carbons, C(2), C(3), and C(2*), all lie on the same side of the Pd_3 plane as the S(1) atom; this is in contrast to the conformational preference noted above for $M_3(\mu\text{-dppm})_3$ complexes with an equilateral M_3 triangle. The conformation found for **3a** presumably serves to minimize intraion phenyl···phenyl interactions. The shortest interion distance between the Pd_3S core of **3a** and the SCN^- counter ion (which is slightly disordered about a mirror plane) is greater than 6 Å, unlike the situation noted above for **2b**. The dichloroethane molecules of solvation fill what would have been voids in the crystal lattice, are only loosely entrapped, and are disordered.

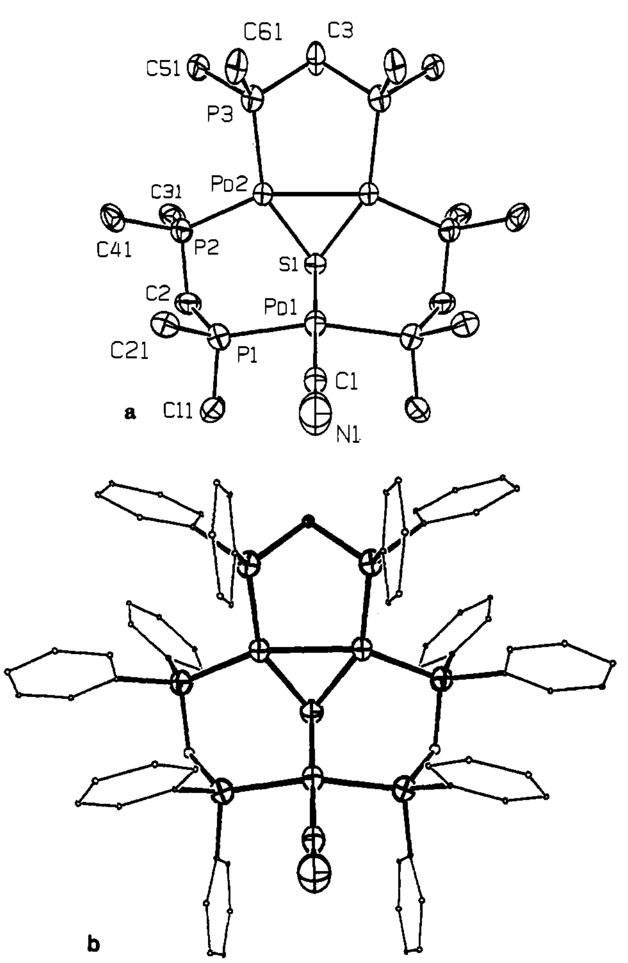

Figure 3. View of the core of **3a** with only the phenyl carbon bonded to phosphorus shown for each phenyl ring and the crystallographic numbering scheme. Phenyl rings are numbered C*n*1–C*n*6, *n* = 1–6. Ellipsoids are at the 50% probability level. (b) View similar to part a but with all carbon atoms shown as small spheres of arbitrary radii.

The metal–metal bonded fragment of **3a** of general formula $[M_2(\mu\text{-S})L_4]$ has been observed previously in such complexes as $[Pt_2(\mu\text{-S})(CO)(PPh_3)_3]$ and $[Pt_2(\mu\text{-S})(CS)(PPh_3)(Ph_2PCH_2CH_2PPh_2)]$ and is also related to the $[Pd_2(\mu\text{-PPh}_2)(\mu\text{-}$

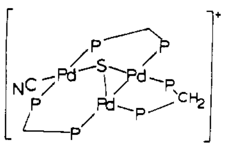

IV

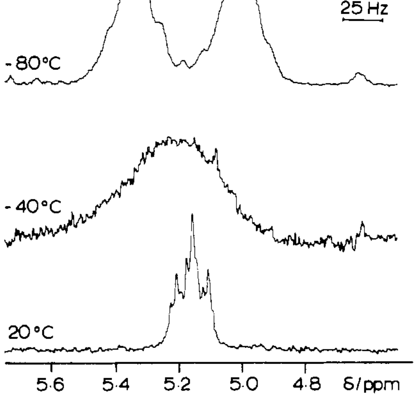

Figure 4. Variable-temperature ^1H NMR spectra (200 MHz) of complex **3a**, showing only the resonance of the P_2CH_2 protons of the unique dppm ligand (solvent, acetone-d_6).

dppm)$(PPh_3)_2]^+$ ion.[4-6,25] In this case the bridging sulfide ligand acts as a 2-electron donor to a third palladium center in the $[Pd^{II}(CN)L_2]^+$ fragment. The μ-dppm ligands are probably responsible for holding the trinuclear unit together during the oxidative addition.

The addition of thiocyanate to **1b** to give **2b** formally increases the electron count of the cluster from 42 to 44 electrons, but this has very little effect on the Pt–Pt distances, as discussed earlier. The overall reaction of **1a** to **3a** causes an increase in cluster electron count from 42 to 46 electrons, and now there is a fundamental change in the nature of the cluster. Each palladium center maintains a 16-electron configuration in both **1a** and **3a**, and to achieve this favored electron count, **1a** requires three Pd–Pd bonds but **3a** requires only one. Thus the oxidative addition leads to opening up of the cluster.[8] In complex **1a** the average oxidation state of palladium is $+^2/_3$ but in **3a** it is $+^4/_3$ as a result of the oxidative addition. In **1a** all palladiums are equivalent whereas in **3a** there are clearly two Pd(I) centers and one Pd(II) center.

There is no evidence for weakening of the S–C bond of thiocyanate in **2b**, but a mechanism of oxidative addition involving strengthening of the $Pt_3(\mu_3\text{-}S)$ linkage with loss of CN^- followed by rapid displacement of CO by CN^- is envisaged. A concerted mechanism should give a product with the sulfide and cyanide ligands mutually cis, but since such a complex could rapidly isomerize to the observed trans structure, this mechanism is also possible. The reaction of **2b** to give **3b** is much slower than in the palladium case, for reasons that are not yet understood.

Evidence for Inversion of the $Pd_3(\mu_3\text{-}S)$ Group of 3a. The $^{31}P\{^1H\}$ NMR spectrum of **3a** gave three complex resonances at $\delta(P) = 23.8$, 0.9, and -4.4 as expected for the structure determined by X-ray diffraction. The spectrum was interpreted and simulated satisfactorily in terms of an AA′MM′XX′ spin system, and the derived parameters are given in the Experimental Section.

The ^1H NMR spectrum of **3a** at room temperature contained two resonances in 2:1 intensity ratio due to the CH_2P_2 protons of the dppm ligands bridging the Pd(II)–Pd(I) and Pd(I)–Pd(I) edges at $\delta = 3.77$ [q, $J_{obsd}(PH) = 4$ Hz] and 5.15 [tt, $^2J(PH) = 10$ Hz, $^4J(PH) = 3$ Hz]. This was not expected since there is no plane of symmetry containing the $Pd_3(dppm)_3$ unit and so each of the above resonances should appear as an AB quartet, due to nonequivalent $CH^aH^bP_2$ protons. At low temperature (−80 °C) the resonance at 5.15 ppm had split into the expected AB quartet [$\delta(H^a) = 5.34$, $\delta(H^b) = 5.00$, $^2J(H^aH^b) = 14$ Hz], and the resonance at 3.77 ppm was greatly broadened (Figure 4). These results indicate that **3a** is fluxional and undergoes rapid inversion of the $Pd_3(\mu_3\text{-}S)$ unit to generate an effective plane of symmetry containing the $Pd_3(dppm)_3$ unit at room temperature. The activation energy for inversion in acetone-d_6, based on $\Delta\nu = 67$ Hz at 200 MHz and $T_c = -40$ °C, was estimated to be $\Delta G^{\ddagger} \sim 47$ kJ mol^{-1}. The transition state presumably has a planar $Pd_3(\mu_3\text{-}S)$ unit.

Table III. Crystal Data and Structure Analysis Parameters for $[Pt_3(SCN)(\mu_3\text{-}CO)(\mu\text{-dppm})_3][PF_6]\cdot 2(CH_3)_2CO$ and for $[Pd_3(\mu_3\text{-}S)(CN)(\mu\text{-dppm})_3][SCN]\cdot 3C_2H_4Cl_2$

	[**2b**]$[PF_6]\cdot 2(CH_3)_2CO$	[**3a**][SCN]$\cdot 3C_2H_4Cl_2$
empirical formula	$C_{83}H_{78}F_6NO_3P_7Pt_3S$	$C_{83}H_{78}Cl_6Pd_3N_2P_6S_2$
fw	2085.68	1885.45
space group	$P2_1/n$	*Pnma*
a, Å	16.125 (1)	24.110 (7)
b, Å	26.622 (2)	21.652 (5)
c, Å	19.403 (1)	16.126 (3)
β, deg	104.45 (1)	
V, Å^3	8066 (1)	8418 (3)
Z	4	4
d(calcd), g cm^{-3}	1.718	1.49
cryst dimens, mm	0.43 × 0.35 × 0.15	0.21 × 0.31 × 0.34
μ(Mo Kα), cm^{-1}	54.7	10.2
temp of data collcn,[a] °C	22	21
μ-scan width in $\omega/2\theta$ for data collcn	$0.70 + 0.35(\tan\theta)$	$0.60 + 0.35(\tan\theta)$
data collcn range	$2 \le \theta \le 23$ $23 \le \theta < 24.5$[b]	$2 \le \theta \le 24°$
no. of std reflcns	2	3
measd	no decay	no decay
empirical transmission factors (on $\|F\|$)	0.83–1.27	no correction made
R	0.0413	0.049
R_w	0.0530	0.074
S	2.92	2.39
no. of indep reflcns	12896	4504
no. of reflcns ($I > 3\sigma(I)$)	7057	3423
no. of params	295	445
max $\|\Delta\rho\|_{final}$, e Å^{-3}	1.75	1.10

[a] Data were collected on a CAD-4 diffractometer equipped with graphite monochromators and using Mo Kα radiation ($\lambda = 0.71069$ Å). [b] Data collection of this second shell was discontinued when it became obvious that very few reflections had intensities significantly above background.

Activation energies similar to that given above have been determined for inversion at sulfur in complexes containing the functional groups $M\text{-}SR_2$ and $M_2(\mu\text{-}SR)$ but this appears to be the first evidence for inversion at sulfur in $M_3(\mu_3\text{-}S)$ derivatives.[26]

Conclusions

The oxidative addition of thiocyanate described above has several interesting features. This reaction of thiocyanate to give sulfide and cyanide has not been observed in mononuclear complexes and so probably represents an example where activation by more than one metal center is necessary. It is suggested that the strength of the incipient $M_3(\mu_3\text{-}S)$ unit stabilizes the transition state in which the strong C–S bond of thiocyanate is cleaved. It has recently been shown that *photolysis* of $[Pd(PPr_3)_2(NCS)_2]$ in CH_3CN solution gives $[Pd_2(PPr_3)_3(NCS)(SCN)_2(\mu\text{-}CN)]$.[27] It was suggested that the CN^- ligand was formed from CH_3CN solvent, since no precedents for formation of CN^- from NCS^- were known and since the product was not formed in methanol solvent. Perhaps the derivation of CN^- from SCN^- in this case should now be reconsidered.

The use of μ-dppm ligands to lock together two metal atoms in binuclear complexes is now well established. The new chemistry

---

(25) Hadj-Bagheri, N.; Dixon, K. R.; Vefghi, R., personal communication.

(26) Abel, E. W.; Bhargava, S. K.; Orrell, K. G. *Prog. Inorg. Chem.* **1984**, *32*, 1.

(27) Bombieri, G.; Bruno, G; Cusumano, M.; Guglielmo, G.; Ricevuto, V. *Polyhedron* **1985**, *4*, 1365.

Table IV. Fractional Atomic Coordinates[a] and Isotropic Displacement Parameters for $[Pt_3(SCN)(\mu_3\text{-}CO)(\mu\text{-dppm})_3][PF_6]\cdot 2(CH_3)_2CO$

	x/a	y/b	z/c	U, Å^2		x/a	y/b	z/c	U, Å^2
Pt(1)	0.18798 (3)	0.23220 (2)	0.44681 (3)	0.032[b]	C(E3)	0.0162 (7)	0.3722 (6)	0.1118 (8)	0.100 (6)
Pt(2)	0.20003 (3)	0.28116 (2)	0.33261 (3)	0.035	C(E4)	0.0542 (7)	0.4105 (6)	0.0828 (9)	0.110 (7)
Pt(3)	0.19004 (3)	0.18279 (2)	0.33019 (3)	0.034	C(E5)	0.1422 (7)	0.4123 (4)	0.0947 (4)	0.112 (7)
P(1)	0.1880 (2)	0.3042 (1)	0.5136 (2)	0.036	C(E6)	0.1921 (7)	0.3758 (7)	0.1355 (10)	0.085 (6)
P(2)	0.2329 (2)	0.3570 (1)	0.3889 (2)	0.037	C(F1)	0.3250 (9)	0.2934 (5)	0.2113 (8)	0.056 (4)
P(3)	0.2158 (2)	0.2885 (1)	0.2200 (2)	0.045	C(F2)	0.3444 (17)	0.2944 (10)	0.1460 (13)	0.109 (8)
P(4)	0.2088 (2)	0.1741 (1)	0.2182 (2)	0.043	C(F3)	0.4283 (23)	0.2995 (12)	0.1422 (17)	0.157 (10)
P(5)	0.2073 (3)	0.1053 (1)	0.3819 (2)	0.045	C(F4)	0.4929 (18)	0.3037 (10)	0.2039 (16)	0.128 (9)
P(6)	0.1696 (2)	0.1606 (1)	0.5083 (2)	0.039	C(F5)	0.4735 (15)	0.3027 (8)	0.2692 (13)	0.107 (7)
P(7)	−0.2659 (3)	0.4919 (2)	0.3858 (3)	0.102	C(F6)	0.3895 (11)	0.2976 (7)	0.2729 (9)	0.064 (5)
S	0.3534 (3)	0.2197 (2)	0.4540 (2)	0.073	C(G1)	0.3191 (8)	0.1654 (6)	0.2135 (12)	0.056 (4)
F(1)	−0.3468 (10)	0.4847 (10)	0.3276 (7)	0.218 (8)[c]	C(G2)	0.3829 (11)	0.1601 (4)	0.2754 (8)	0.066 (4)
F(2)	−0.2150 (12)	0.4662 (3)	0.3404 (11)	0.295 (11)	C(G3)	0.4661 (10)	0.1510 (7)	0.2721 (7)	0.101 (6)
F(3)	−0.2804 (8)	0.4419 (3)	0.4175 (8)	0.351 (14)	C(G4)	0.4855 (7)	0.1473 (5)	0.2070 (10)	0.108 (7)
F(4)	−0.1849 (10)	0.4991 (10)	0.4441 (7)	0.223 (8)	C(G5)	0.4217 (11)	0.1526 (4)	0.1451 (7)	0.125 (8)
F(5)	−0.2513 (8)	0.5419 (3)	0.3541 (8)	0.342 (14)	C(G6)	0.3385 (10)	0.1617 (7)	0.1483 (9)	0.091 (6)
F(6)	−0.3167 (12)	0.5176 (3)	0.4312 (11)	0.315 (13)	C(H1)	0.1426 (12)	0.1261 (6)	0.1634 (4)	0.051 (4)
O	0.0237 (6)	0.2379 (3)	0.3271 (5)	0.051 (2)	C(H2)	0.0553 (12)	0.1298 (3)	0.1552 (9)	0.057 (4)
O(S1)	0.716 (2)	0.023 (1)	0.433 (1)	0.226 (7)	C(H3)	0.0014 (7)	0.0939 (5)	0.1166 (8)	0.078 (5)
O(S2)	0.243 (2)	0.253 (2)	0.954 (2)	0.341 (11)	C(H4)	0.0347 (10)	0.0544 (5)	0.0862 (4)	0.086 (6)
N	0.4539 (11)	0.2687 (6)	0.5686 (10)	0.118 (6)	C(H5)	0.1220 (10)	0.0507 (3)	0.0944 (9)	0.086 (6)
C(1)	0.2598 (8)	0.3484 (4)	0.4861 (7)	0.038 (3)	C(H6)	0.1760 (7)	0.0865 (6)	0.1330 (8)	0.073 (5)
C(2)	0.1733 (8)	0.2309 (5)	0.1671 (7)	0.049 (3)	C(I1)	0.2953 (10)	0.0685 (5)	0.3647 (11)	0.048 (4)
C(3)	0.2329 (8)	0.1105 (5)	0.4800 (7)	0.046 (4)	C(I2)	0.2806 (8)	0.0419 (7)	0.3018 (8)	0.068 (5)
C(4)	0.0971 (8)	0.2356 (5)	0.3524 (7)	0.041 (3)	C(I3)	0.3478 (12)	0.0185 (5)	0.2824 (6)	0.085 (5)
C(5)	0.4104 (11)	0.2477 (6)	0.5191 (10)	0.073 (5)	C(I4)	0.4296 (8)	0.0217 (4)	0.3259 (9)	0.093 (6)
C(A1)	0.2254 (10)	0.3021 (6)	0.6103 (4)	0.042 (3)	C(I5)	0.4443 (9)	0.0484 (7)	0.3888 (7)	0.099 (6)
C(A2)	0.3075 (7)	0.3158 (2)	0.6458 (6)	0.061 (4)	C(I6)	0.3771 (13)	0.0717 (5)	0.4082 (7)	0.071 (5)
C(A3)	0.3327 (8)	0.3130 (6)	0.7191 (6)	0.078 (5)	C(J1)	0.1171 (10)	0.0633 (7)	0.3573 (5)	0.049 (4)
C(A4)	0.2759 (9)	0.2966 (5)	0.7569 (4)	0.090 (6)	C(J2)	0.1229 (7)	0.0139 (7)	0.3794 (9)	0.066 (5)
C(A5)	0.1938 (5)	0.2830 (3)	0.7214 (6)	0.079 (5)	C(J3)	0.0524 (8)	−0.0172 (4)	0.3604 (8)	0.078 (5)
C(A6)	0.1685 (9)	0.2857 (7)	0.6481 (6)	0.075 (5)	C(J4)	−0.0240 (9)	0.0011 (5)	0.3191 (5)	0.103 (7)
C(B1)	0.0863 (7)	0.3376 (6)	0.5002 (10)	0.039 (3)	C(J5)	−0.0298 (7)	0.0505 (7)	0.2969 (9)	0.104 (7)
C(B2)	0.0118 (11)	0.3164 (3)	0.4599 (9)	0.056 (4)	C(J6)	0.0407 (9)	0.0816 (3)	0.3160 (8)	0.065 (4)
C(B3)	−0.0640 (9)	0.3430 (6)	0.4468 (4)	0.085 (6)	C(K1)	0.0594 (8)	0.1387 (7)	0.4916 (7)	0.046 (3)
C(B4)	−0.0653 (6)	0.3908 (5)	0.4740 (8)	0.088 (6)	C(K2)	0.0404 (8)	0.0885 (7)	0.4961 (11)	0.070 (5)
C(B5)	0.0092 (11)	0.4120 (4)	0.5143 (7)	0.077 (5)	C(K3)	−0.0438 (10)	0.0730 (3)	0.4820 (8)	0.095 (6)
C(B6)	0.0850 (9)	0.3854 (7)	0.5274 (6)	0.067 (5)	C(K4)	−0.1090 (7)	0.1077 (6)	0.4633 (7)	0.102 (7)
C(C1)	0.1485 (7)	0.4044 (5)	0.3700 (10)	0.040 (3)	C(K5)	−0.0901 (8)	0.1580 (6)	0.4588 (10)	0.111 (7)
C(C2)	0.1635 (8)	0.4517 (7)	0.3997 (6)	0.049 (4)	C(K6)	−0.0058 (10)	0.1734 (4)	0.4729 (7)	0.076 (5)
C(C3)	0.0991 (10)	0.4872 (4)	0.3863 (6)	0.064 (4)	C(L1)	0.2119 (9)	0.1571 (6)	0.6044 (5)	0.047 (4)
C(C4)	0.0197 (7)	0.4754 (4)	0.3432 (8)	0.075 (5)	C(L2)	0.1687 (9)	0.1331 (6)	0.6480 (6)	0.052 (4)
C(C5)	0.0046 (8)	0.4281 (6)	0.3135 (5)	0.069 (5)	C(L3)	0.2055 (5)	0.1294 (3)	0.7201 (5)	0.088 (6)
C(C6)	0.0690 (11)	0.3926 (3)	0.3269 (8)	0.057 (4)	C(L4)	0.2854 (8)	0.1497 (5)	0.7486 (4)	0.075 (5)
C(D1)	0.3248 (5)	0.3906 (4)	0.3730 (6)	0.038 (3)	C(L5)	0.3286 (7)	0.1737 (5)	0.7050 (5)	0.077 (5)
C(D2)	0.4061 (6)	0.3873 (4)	0.4174 (5)	0.064 (4)	C(L6)	0.2918 (6)	0.1775 (3)	0.6329 (4)	0.060 (4)
C(D3)	0.4743 (7)	0.4093 (6)	0.3978 (7)	0.072 (5)	C(S11)	0.698 (1)	0.021 (1)	0.368 (1)	0.226[d]
C(D4)	0.4612 (5)	0.4345 (4)	0.3338 (5)	0.075 (5)	C(S12)	0.690 (3)	−0.029 (1)	0.330 (2)	0.226
C(D5)	0.3798 (6)	0.4378 (5)	0.2894 (6)	0.079 (5)	C(S13)	0.684 (2)	0.069 (1)	0.325 (2)	0.226
C(D6)	0.3117 (7)	0.4158 (6)	0.3090 (7)	0.058 (4)	C(S21)	0.168 (2)	0.243 (1)	0.954 (1)	0.341
C(E1)	0.1542 (8)	0.3375 (7)	0.1645 (11)	0.052 (4)	C(S22)	0.105 (3)	0.285 (1)	0.952 (4)	0.341
C(E2)	0.0662 (8)	0.3357 (3)	0.1526 (6)	0.072 (5)	C(S23)	0.141 (3)	0.183 (1)	0.957 (2)	0.341

[a] Group constraints: C_6H_5 rings have C–C = 1.380 Å, C–H = 0.96 Å, and ∠C–C–C = 120°; $[PF_6]^-$ has P–F = 1.530 Å and ∠F–P–F = 90 or 180°; $(CH_3)_2CO$ molecules have C–C = 1.516 Å, C–O = 1.230 Å, and ∠C–C–C = ∠C–C–O = 120°. [b] For Pt, P, and S atoms = $^1/_3\sum_{i=1}^{3}\sum_{j=1}^{3}U_{ij}a^*_i a^*_j a_i \cdot a_j$. [c] For F, O, N, and C atoms the isotropic temperature factor expression was $\exp(-8\pi^2 U(\sin^2\theta)/\lambda^2)$. [d] U for C(Sij) = U for O(Si) (j = 1, 3; i = 1, 2).

described here shows that the triangular M_3 core may be similarly stabilized against fragmentation and suggests that a large number of further reactions of the M_3 triangles of **1a** and **1b** may be possible. In contrast, most reactions of platinum clusters, such as $[Pt_3(\mu\text{-}CO)_3L_3]$, containing monodentate phosphine ligands, L, lead to fragmentation and so the organometallic chemistry of the Pt_3 unit has been developed to only a limited extent.[28,29] For example, reaction with CS_2 has recently been shown to give $[Pt_2(\mu\text{-}CS_2)_2L_2]$ (L = P-*t*-Bu$_2$Ph) rather than a trinuclear derivative.[30] The μ-dppm ligands in complexes **1–3** prevent such fragmentation and so allow a clearer picture of the reaction course to be obtained. Further work along these lines is in progress.

Experimental Section

$^1H\{^{31}P\}$ NMR spectra were run on a Varian XL100 NMR spectrometer while ^1H NMR spectra were collected on both the Varian XL100 and XL200 spectrometers. $^{31}P\{^1H\}$ and $^{195}Pt\{^1H\}$ spectra were run on a Varian XL300 NMR spectrometer (the $^{195}Pt\{^1H\}$ NMR spectrum being run at 64.274 MHz). The external references were $(MeO)_3PO$ in acetone for ^{31}P and aqueous $K_2[PtCl_4]$ for ^{195}Pt NMR. IR spectra were recorded on a Beckman Acculab 4 IR spectrometer as Nujol mulls. UV–visible spectra were run on a Cary 112 spectrometer.

Reaction of $[Pd_3(\mu_3\text{-}CO)(\mu\text{-dppm})_3][CF_3CO_2]_2$ with KSCN. $[Pd_3(\mu_3\text{-}CO)(\mu\text{-dppm})_3][CF_3CO_2]_2$ (0.113 mmol) was reacted with KSCN (0.381 mmol) in acetone (~40 mL) under N_2 for 24 h. The volume of the solution was then reduced to ~10 mL and the solution was cooled to 0 °C. The red crystalline product was filtered and dried in vacuo. Yield: 38%. Anal. Calcd for $[Pd_3S(CN)(dppm)_3]SCN$: C, 58.2; H, 4.19; N, 1.76. Found: C, 57.3; H, 3.69; N, 2.11. NMR in $(CD_3)_2CO$: ^1H, δ 3.77 [quintet, 4 H, $J_{obsd}(PH)$ = 3.8 Hz, CH_2P_2], 5.15 [tt, 2 H, $^2J(PH)$ = 10.1 Hz, $^4J(PH)$ = 3.1 Hz, CH_2P_2]; ^{31}P, δ 23.8 [m, $^2J(P^aP^{a\prime})$ = 450 Hz, $^2J(P^aP^m)$ = 65 Hz, $^3J(P^aP^{m\prime})$ = 8 Hz, $^3J(P^aP^x)$ = 8 Hz, $^3J(P^aP^{x\prime})$ = 5 Hz, P^a], 0.9 [m, $^3J(P^mP^{m\prime})$ = 175 Hz, $^2J(P^mP^x)$ = 9 Hz, $^3J(P^mP^{x\prime})$ = 15

---

(28) Mingos, D. M. P.; Wardle, R. W. M. *Transition Met. Chem. (Weinheim, Ger.)* **1985**, *10*, 441.

(29) Eremko, N. K.; Mednikov, E. G.; Kurasov, S. S. *Russ. Chem. Rev. (Engl. Transl.)* **1985**, *54*, 394.

(30) Farrar, D. H.; Gukathasan, R. R.; Morris, S. A. *Inorg. Chem.* **1984**, *23*, 3258.

Hz, P^m], −4.4 [m, $^2J(P^xP^{x'})$ = 5 Hz, P^x]. IR (Nujol): ν(CN) = 2070 cm^{-1}.

Single crystals of the sample were grown by slow diffusion of pentane into a 1,2-dichloroethane solution of the product.

UV–Visible and NMR Spectral Studies of the Formation of [$Pd_3(\mu_3$-S)(CN)(μ-dppm)$_3$][SCN]. [$Pd_3(\mu_3$-CO)(μ-dppm)$_3$][CF_3CO_2]$_2$ (~0.048 mmol) was dissolved in MeOH (50 mL). A 2-mL aliquot of this solution was pipetted into a 10-mL volumetric flask. In two separate experiments, either 3 or 6 mL of a 1.6×10^{-4} M solution of KSCN in MeOH was added to the 10-mL volumetric flask, and the resulting solution was then diluted with MeOH to the 10-mL volume. The reaction was monitored by changes in the UV–visible spectra of the solution in a 1-cm cuvette over a 72-h period at 22 °C.

Addition of 1 mol of SCN^- to a solution of **1a** in acetone-d_6 led to a shift in the ^{31}P resonance to −11.3 ppm.

Reaction of [$Pt_3(\mu_3$-CO)(μ-dppm)$_3$][PF_6]$_2$ with KSCN. [$Pt_3(\mu_3$-CO)(μ-dppm)$_3$][PF_6]$_2$ (0.049 mmol) was reacted with KSCN (0.169 mmol) in acetone (25 mL) under N_2 overnight. To ensure isolation of a pure hexafluorophosphate salt this solution was then added to a methanol solution of NH_4PF_6 (2.785 mmole). Addition of H_2O followed by removal of acetone under vacuum gave a flocculent precipitate, which was isolated by filtration, washed with H_2O and dried in vacuo. Yield: 83.8%. NMR in $(CD_3)_2CO$: ^1H, δ 5.84 [m, ^2J(HH) = 14 Hz, ^3J(PtH) = 52 Hz, CH^aH^b), 5.61 [m, ^2J(HH) = 14 Hz, ^3J(PtH) = 44 Hz, CH^aH^b); ^{31}P, δ −15.3 [s, ^1J(PtP) = 3670 Hz, ^3J(PP) = 165 Hz]; ^{195}Pt, δ −2713 [t, ^1J(PtP) = 3670 Hz, ^1J(PtPt) = 480 Hz]. IR (Nujol): ν(NCS) = 2070, ν(CO) = 1810 cm^{-1}.

One sample was recrystallized from acetone by slow diffusion of pentane. Anal. Calcd for [$Pt_3(\mu_3$-SCN)(μ_3-CO)(μ-dppm)$_3$][PF_6]·$2Me_2CO$: C, 47.80; H, 3.78; N, 0.67. Found: C, 47.92; H, 3.97; N, 0.50.

X-ray Analysis of [Pt_3(SCN)(μ_3-CO)(μ-dppm)$_3$][PF_6]·2$(CH_3)_2CO$. The crystal specimen was a transparent orange plate, mounted in air. The final cell dimensions (Table III) are based on a least-squares fit to the setting angles of 23 reflections with $14 < \theta(\text{Mo } K\alpha) < 18°$.[31] The space group was established from the systematic absences and confirmed by our successful analysis. Corrections were made for Lorentz–polarization effects, assuming an ideally imperfect monochromator crystal, and for absorption by using the empirical method of Walker and Stuart.[32]

The Pt positions were derived from the Patterson function and those of the remaining non-hydrogen atoms from subsequent difference syntheses. In the final calculations contributions were included for the scattering of all hydrogen atoms except those of the two acetone molecules. Hydrogen positions were deduced geometrically, assuming a C–H bond length of 0.96 Å and that $U_{iso}(H) = U_{iso}(C)$. The final structural model (Tables I and IV), was derived by full-matrix least-squares refinement on F with $w = \sigma(F)^{-2}$. The number of refined parameters was limited to 295 by an extensive use of constraints. The 12 C_6H_5 rings, the $[PF_6]^-$ anion, and the two acetone molecules were treated as rigid groups with the geometries specified in Table IV. The shifts of the methylenic C atoms were applied to the corresponding methylene H atoms. Anisotropic displacement parameters were adjusted only for the Pt, P, and S atoms. For the other non-H atoms U_{iso} parameters were refined, except for each acetone molecule for which a single U_{iso} parameter, common to the C and O atoms, was adjusted. The final difference synthesis showed only random fluctuations, with $|\Delta\rho| < 1.0$ e $Å^{-3}$, except in the region of the $[PF_6]^-$ anion, where a number of features in the range 1.0–1.8 e $Å^{-3}$ seemed more consistent with a slight positional disorder of the F atoms rather than with a failure to allow for their anisotropic thermal motion. Consistent with this, mean values of $w\Delta^2$ showed no variation with $|F_o|$ but increased at low values of $(\sin \theta)/\lambda$.

Neutral atom scattering factors and complex anomalous dispersion corrections (for all non-H atoms) were taken from ref 33. Calculations were carried out on a GOULD 3227 32-bit minicomputer using the locally developed GX program package.[34]

X-ray Analysis of [$Pd_3(\mu_3$-S)(CN)(μ-dppm)$_3$][SCN]·$3C_2H_4Cl_2$. Crystalline material suitable for diffraction work was obtained by slow crystallization from dichloroethane. The red crystals so obtained lose dichloroethane of solvation slowly on standing. For the data collection a small crystal (see Talbe III) was selected and coated completely with epoxy glue to prevent solvent loss. The cell data and orientation matrix were determined from the setting angles of 25 reflections with $10° \leq \theta \leq 13°$. The systematic absences (0*kl* absent if $k + l = 2n + 1$; *hk*0 absent if $h = 2n + 1$) allow the space group to be either *Pnma* or *Pn*2^1*a*. *Pnma* was chosen and confirmed by the analysis. Intensity data were corrected for Lorentz and polarization effects but not for absorption.

Table V. Positional Parameters and Their Estimated Standard Deviations for **3a**

atom	*x*	*y*	*z*
Pd(1)	0.14898 (4)	0.25	0.64662 (6)
Pd(2)	0.02803 (3)	0.19044 (3)	0.73741 (4)
S(1)	0.0547 (1)	0.25	0.6264 (2)
P(1)	0.1547 (1)	0.1441 (1)	0.6259 (2)
P(2)	0.0391 (1)	0.0950 (1)	0.6773 (2)
P(3)	−0.0158 (1)	0.1813 (1)	0.8613 (2)
N(1)	0.2744 (5)	0.25	0.6871 (9)
C(1)	0.2325 (5)	0.25	0.6736 (8)
C(2)	0.0912 (4)	0.1008 (4)	0.5955 (5)
C(3)	−0.0585 (5)	0.25	0.8827 (8)
C(11)	0.1999 (4)	0.1348 (4)	0.5360 (6)
C(12)	0.1789 (4)	0.1428 (6)	0.4572 (7)
C(13)	0.2134 (5)	0.1438 (8)	0.3886 (7)
C(14)	0.2693 (5)	0.1365 (6)	0.4012 (7)
C(15)	0.2897 (5)	0.1282 (8)	0.4769 (8)
C(16)	0.2564 (4)	0.1263 (7)	0.5449 (7)
C(21)	0.1849 (4)	0.0972 (4)	0.7065 (5)
C(22)	0.1974 (4)	0.0360 (4)	0.6938 (6)
C(23)	0.2196 (5)	0.0010 (5)	0.7585 (7)
C(24)	0.2283 (4)	0.0276 (5)	0.8347 (7)
C(25)	0.2167 (4)	0.0886 (5)	0.8492 (6)
C(26)	0.1946 (4)	0.1241 (4)	0.7836 (6)
C(31)	−0.0229 (4)	0.0731 (4)	0.6207 (6)
C(32)	−0.0588 (4)	0.0279 (5)	0.6455 (7)
C(33)	−0.1073 (5)	0.0168 (6)	0.6096 (8)
C(34)	−0.1242 (5)	0.0468 (6)	0.5451 (8)
C(35)	−0.0917 (5)	0.0935 (6)	0.5160 (7)
C(36)	−0.0402 (4)	0.1075 (5)	0.5550 (7)
C(41)	0.0589 (4)	0.0253 (4)	0.7307 (5)
C(42)	0.0629 (4)	−0.0300 (4)	0.6914 (6)
C(43)	0.0783 (5)	−0.0832 (4)	0.7355 (7)
C(44)	0.0908 (4)	−0.0811 (5)	0.8167 (7)
C(45)	0.0879 (5)	−0.0262 (5)	0.8558 (6)
C(46)	0.0716 (4)	0.0270 (4)	0.8142 (6)
C(51)	−0.0661 (4)	0.1180 (4)	0.8643 (5)
C(52)	−0.0550 (4)	0.0621 (4)	0.9068 (6)
C(53)	−0.0904 (5)	0.0130 (4)	0.8989 (7)
C(54)	−0.1375 (5)	0.0184 (5)	0.8520 (8)
C(55)	−0.1482 (4)	0.0696 (5)	0.8095 (8)
C(56)	−0.1139 (4)	0.1211 (5)	0.8170 (6)
C(61)	0.0250 (4)	0.1719 (4)	0.9543 (6)
C(62)	0.0817 (4)	0.1686 (4)	0.9490 (6)
C(63)	0.1143 (4)	0.1615 (5)	1.0217 (7)
C(64)	0.0887 (5)	0.1573 (5)	1.0959 (6)
C(65)	0.0321 (4)	0.1606 (6)	1.1032 (6)
C(66)	0.0002 (5)	0.1694 (5)	1.0319 (6)
Cl(11)	0.2320 (2)	0.25	0.9267 (3)
Cl(12)	0.4025 (2)	0.25	0.8525 (4)
Cl(2)	0.0490 (2)	0.1523 (2)	0.3455 (3)
Cl(31)	0.2534 (4)	0.1373 (4)	0.1275 (6)
Cl(32)	0.3089 (8)	0.1833 (8)	0.160 (1)
S(200)	0.4045 (4)	0.25	0.2581 (7)
N(200)	0.378	0.25	0.423
C(200)	0.389	0.25	0.354
C(111)	0.295	0.225	0.900
C(112)	0.339	0.225	0.881
C(221)	0.055	0.228	0.312
C(222)	0.041	0.228	0.376

The coordinates of the unique Pd atoms were determined from a careful analysis of the three-dimensional Patterson function, and the coordinates of the remaining atoms were found from subsequent rounds of structure factor and difference Fourier calculations. While the coordinates for the non-hydrogen atoms of cation **3a** (which lies on a crystallographic mirror plane) were readily obtained, the SCN^- counterion appeared, from the diffuse peaks on difference maps, to be disordered about a mirror plane. Three different locations for dichloroethane molecules of solvation could also be discerned.

At location one, the Cl atoms lie on either side of a mirror plane and the CH_2–CH_2 groups are disordered over two sites. In the second solvent molecule, both Cl atoms lie on the mirror plane and the carbons are

---

(31) De Boer, J. L.; Duisenberg, A. J. M. *Enraf-Nonius CAD4F Diffractometer Software Update Feb-84*; Enraf-Nonius: Groningen and Utrecht, The Netherlands, 1984.

(32) Walker, N.; Stuart, D. *Acta Crystallogr., Sect. A: Found. Crystallogr.* **1983**, *A39*, 158.

(33) *International Tables for X-ray Crystallography*; Kynoch: Birmingham, England, 1974; Vol. IV, pp. 99 and 149.

(34) Mallinson, P. R.; Muir, K. W. *J. Appl. Crystallogr.* **1985**, *18*, 51.

disordered about two mirror related sites. The disorder of the third solvent molecule is more complex; the chlorine atoms lie on either side of a mirror plane and are disordered over two sites. The carbon atoms of this molecule are disordered over several sites and were not located.

In the full-matrix least-squares refinement the coordinates of the C atoms of the disordered solvent molecules were positioned from difference maps, and the C and N atom of the SCN^- anion were derived from geometrical considerations and were not refined. Isotropic refinement was followed by anisotropic refinement, and after inclusion of hydrogen atoms (from geometry considerations), the refinement converged with R = 0.049 (see Table III), and a maximum shift/error ratio of 0.04.

As a check that the space group had been correctly chosen, coordinates were derived for the complete structure in the alternative noncentrosymmetric space group $Pn2_1a$ and a new refinement process was begun. No significant improvement in parameter values or R was noted, and in spite of a damped refinement, several cation temperature factors that had behaved reasonably on the *Pnma* refinement moved to nonsensible values. It was concluded that the true space group is *Pnma* with the cation **3a** lying on a mirror plane.

The final difference synthesis in *Pnma* had maxima of 1.1 e $Å^{-3}$ in the volume element of the dichloroethane molecule, which was severely disordered, and no other chemically significant features. In the refinement, weights were based on counting statistics ($w = 1/\sigma(F)^2$) and scattering factors were taken from ref 33. All calculations were performed on a PDP11/73 computer using the SDP system of programs.[34] Final fractional coordinates for non-hydrogen atoms are in Table V. Lists of anisotropic thermal parameters, all bond lengths and angles, calculated hydrogen coordinates, and observed and calculated structure amplitudes are available as supplementary material.

Acknowledgment. G.F. and R.J.P. thank the NSERC (Canada) for financial support. Lj.M.-M. and K.W.M. thank the SERC (Great Britain) and the University of Glasgow for grants used to purchase the diffractometer and computer.

Registry No. [**1a**][CF_3CO_2]$_2$, 89189-80-0; [**1b**][PF_6]$_2$, 99642-80-5; [**2b**][PF_6]·2$(CH_3)_2CO$, 104438-46-2; [**3a**][SCN], 104421-85-4; [**3a**]-[SCN]·3$C_2H_4Cl_2$, 104421-88-7; SCN^-, 302-04-5.

Supplementary Material Available: Listings of anisotropic displacement parameters (Table VI), calculated hydrogen atom positions (Table VII), and PCC bond angles (Table VIII) for $[Pt_3(SCN)(\mu_3\text{-}CO)(\mu\text{-}dppm)_3][PF_6]\cdot 2(CH_3)_2CO$ and general temperature factor expressions (Table X), bond distances (Table XI), bond angles (Table XII), and calculated hydrogen atom positions (Table XIII) for $[Pd_3(\mu_3\text{-}S)(CN)(\mu\text{-}dppm)_3][SCN]\cdot 3C_2H_4Cl_2$ (13 pages); listings of final $|F_o|$ and $|F_c|$ values for $[Pt_3(SCN)(\mu_3\text{-}CO)(\mu\text{-}dppm)_3][PF_6]\cdot 2(CH_3)_2CO$ (Table IX) and $[Pd_3(\mu_3\text{-}S)(CN)(\mu\text{-}dppm)_3][SCN]\cdot 3C_2H_4Cl_2$ (Table XIV) (64 pages). Ordering information is given on any current masthead page.

Contribution from the Departments of Chemistry, Boston College, Chestnut Hill, Massachusetts 02167,
and Georgia Institute of Technology, Atlanta, Georgia 30332, Dipartimento di Chimica,
Università di Firenze, 50144 Firenze, Italy, and ISSECC (CNR), 50132 Firenze, Italy

Thermodynamic and Structural Studies of Configurational Isomers of $[Ni(cyclam)]^{2+}$

E. Kent Barefield,*[1a] Antonio Bianchi,[1b] E. Joseph Billo,*[1c] Peter J. Connolly,[1c] Piero Paoletti,*[1d]
Jack S. Summers,[1a] and Donald G. Van Derveer[1a]

Received March 26, 1986

Single-crystal X-ray structures of two new complexes of nickel(II)–cyclam are reported: *cis*-$[Ni(C_{10}H_{24}N_4)(OH_2)_2]Cl_2\cdot 2H_2O$ (298 K; triclinic, space group $P\bar{1}$, a = 13.625 (3) Å, b = 8.0091 (8) Å, c = 9.187 (1) Å, α = 101.31 (1)°, β = 92.86 (2)°, γ = 107.76 (1)°, ρ_{calcd} = 1.437 g cm^{-3} for Z = 2 and M_r = 402.07, R = 0.028, R_w = 0.031) and $[Ni(C_{10}H_{24}N_4)]ZnCl_4$ (173 K; orthorhombic, space group $P4_122$, a = 9.879 (1) Å, c = 18.289 (3) Å, ρ_{calcd} = 1.70 g cm^{-3} for Z = 4 and M_r = 466.26, R = 0.062, R_w = 0.066). Both complexes have the *RRRR* set of nitrogen configurations. Ni–N distances average 2.10 Å in the six-coordinate complex and 1.9 Å in the four-coordinate complex. Thermodynamic parameters for the interconversion of these two isomers and the more stable *RRSS* isomer in aqueous solution have been obtained by microcalorimetric measurements of the heats of dissolution of the solid complexes and from the temperature dependence of the high-spin–low-spin equilibrium, determined spectrophotometrically. The enthalpy change for the reaction *RRRR*-planar(aq) → *RRSS*-planar(aq) is surprisingly small, –0.4 kcal mol^{-1}.

Introduction

The importance of nitrogen configurational isomers in the chemistry of metal complexes of tetraaza macrocyclic ligands is becoming more and more obvious. The involvement of configurational isomers has recently been postulated in mechanistic schemes of formation,[2] substitution,[3] and isomerization.[4] Except in the case of complexes of inert metal ions such as Co(III)[5] the observation of such species is difficult. For the more labile metal ions, extensive ligand N- or C-substitution makes isomerization more sluggish and has permitted the isolation of thermodynamically unstable configurational isomers.[6,7] Using this approach, Barefield and co-workers[8] isolated complexes of Ni(II) with the saturated tetraaza macrocycle tetramethylcyclam (1,4,8,11-tetramethyl-1,4,8,11-tetraazacyclotetradecane) in both the trans-III[9] or *RRSS*[10] and the trans-I or *RSRS* geometries (Figure 1). Recently Moore and co-workers[4] showed that the two isomers equilibrate readily in donor solvents, presumably via an intermediate trans-II (*RSRR*) isomer. The *RSRR* isomer has been detected by NMR.[4,11]

The minimum-energy form of the nickel(II) complex of the unsubstituted cyclam ligand also has the *RRSS* (trans-III) geometry.[12] Recently one of us published a convenient synthesis[13] of *cis*-$[Ni(cyclam)(H_2O)_2]^{2+}$, which contains a folded form of the ligand, and measured the rate of folded-to-planar isomerization over the pH range 1–10. In solutions of high perchlorate concentration the violet octahedral folded complex can be converted to a yellow planar low-spin complex,[14] α-$[Ni(cyclam)](ClO_4)_2$,

---

(1) (a) Georgia Institute of Technology. (b) ISSECC (CNR). (c) Boston College. (d) Università di Firenze.

(2) Hay, R. W.; Norman, P. R. *Inorg. Chim. Acta Lett.* **1980**, *45*, 139. Hertli, L.; Kaden, T. A. *Helv. Chim. Acta* **1981**, *64*, 33.

(3) Richens, D. T.; Adzamli, I. K.; Leupin, P.; Sykes, A. G. *Inorg. Chem.* **1984**, *23*, 3065.

(4) Moore, P.; Sachinidis, J.; Willey, G. R. *J. Chem. Soc., Chem. Commun.* **1983**, 522.

(5) Busch, D. H. *Acc. Chem. Res.* **1978**, *11*, 392.

(6) Alcock, N. W.; Moore, P.; Pierpoint, C. *J. Chem. Soc., Dalton Trans.* **1984**, 2371.

(7) Warner, L. G.; Busch, D. H. *J. Am. Chem. Soc.* **1969**, *91*, 4092.

(8) Wagner, F.; Barefield, E. K. *Inorg. Chem.* **1976**, *15*, 408.

(9) The original synthesis and consideration of the stereochemistry of metal complexes of cyclam was given by: Bosnich, B.; Poon, C. K.; Tobe, M. L. *Inorg. Chem.* **1965**, *4*, 1102. The five possible diastereomeric forms of the metal complex were designated as I–V with cis or trans forms to be indicated as such. The use of Cahn–Prelog–Ingold designation of nitrogen configurations as *RRRR* is not meant to indicate that only one enantiomer is present but rather to indicate the relative stereochemistries of the nitrogen atoms in this diastereomer.

(10) Note that this isomer has sometimes been referred to as the *RSSR* isomer. However, the nitrogen configurations should be designated according to their number in the compound 1,4,8,11-tetraazacyclotetradecane. This would result in the designation *RRSS* (or *SSRR* for the other enantiomer).

(11) Lincoln, S. F.; Pisaniello, D. L.; Coates, J. H.; Hadi, D. A. *Inorg. Chim. Acta Lett.* **1984**, *81*, 9.

(12) Bosnich, B.; Mason, R.; Pauling, P. J.; Robertson, G. B.; Tobe, M. L. *Chem. Commun.* **1965**, *97*.

(13) Billo, E. J. *Inorg. Chem.* **1981**, *20*, 4019.